

IDENTIFICATION OF DYNAMIC BEHAVIOR OF STEAM TURBINE BLADES USING ROTOR VIBRATION MEASUREMENT

V. Vasicek - J. Liska - J. Strnad - J. Jakl

University of West Bohemia in Pilsen, NTIS – European Centre of Excellence
Technicka 2, 306 14, Czech Republic
vasicekv@ntis.zcu.cz, jinliska@ntis.zcu.cz, jastrnad@ntis.zcu.cz, jjakl@ntis.zcu.cz

ABSTRACT

Ensuring the reliability of the steam turbine is fundamental task for a proper operation. Monitoring systems are traditionally used for this purpose. Early detection of initial mechanical change can avoid time and financial losses. The last stage blades of low-pressure turbine can be considered as the critical part in a steam turbine operation. The interaction between steam flow and the blisk causes the mechanical stress acting on the blades. Traditional methods used for monitoring blade dynamic behaviour are contact method represented by strain gauges measurement and non-contact method – blade tip timing. However the installation and operation of such monitoring systems is quite expensive. Rising demand for low-cost monitoring systems led into developing new approach which is presented in this paper. It is based on the use of the standard measurement – relative rotor vibration signal. Using the standard measurement makes this approach potentially interesting for the turbine operators compared to the methods traditionally used. This paper illustrates how this principle can be used in blade state monitoring and early identification of the mechanical change in blade structure. The experimental results measured on an experimental rotor test rig are also presented in the paper to support presented approach.

KEYWORDS

DIAGNOSTICS, BLADES, STEAM TURBINE, ROTOR VIBRATION

NOMENCLATURE

f_b blade excitation frequency
 f_o shaft rotational frequency
 φ_B phase of backward rotating phasor of blisk asymmetry
 φ_F phase of forward rotating phasor of blisk asymmetry
 φ_I blisk vibration phase in imaginary coordinate
 φ_o phase of shaft rotational movement
 φ_R blisk vibration phase in real coordinate
 A_B amplitude of backward rotating phasor of blisk asymmetry
 A_F amplitude of forward rotating phasor of blisk asymmetry
 I blisk vibration amplitude in imaginary coordinate
 R blisk vibration amplitude in real coordinate

INTRODUCTION

The turbomachinery is an energy conversion device, converting mechanical energy to thermal/pressure energy or vice versa (Peng 2007). The example can be the steam turbine. The superheated steam spins the bladed wheels of the turbine generating the electric power. Condition

monitoring of the bladed wheel dynamic behavior is necessary to ensure proper operation of the turbomachinery and should not be avoided.

Traditional method for blade behavior identification is based on strain gauge measurement. However, this approach is not suitable for long-term monitoring. Nowadays, the most common method used for rotating blade monitoring is the so-called blade tip-timing method. However, the cost of the sensors and also the installation costs cause that this method is used only in selected turbines. The goal of this research was to use already available sensors in the turbine and extract as much useful information about the blade behavior in turbine operation as possible. For this purpose the relative rotor vibration signal was used, because according to ISO 20816 it is a standard measurement on a steam turbine.

Recently, a lot of papers dealing with the blade vibration monitoring using relative rotor measurements were published by the paper authors. For example in (Liska et al. 2018) there was introduced that the blade vibration presence in relative rotor vibration signal is in a form of two components – lower sideband and upper sideband – as the result of the amplitude modulation with suppressed carrier. The spectral distribution of those components is rotational frequency \pm blade eigenfrequency. However the detailed explanation what is the exact meaning of those two frequency components have still not been published yet. This will be described in this paper and validated by experiments made using experimental rotor test rig.

THEORY BACKGROUND

The principle of blade vibration propagation into shaft vibration is described in detail in this chapter. The axial displacement of a blade (A in Figure 1) causes a tension acting on a blade root. This tension causes bending moment acting on a shaft in a blade root (B in Figure 1) forcing the shaft to bend. The radial shaft vibration can be measured along the shaft (C in Figure 1) except the place of wave nodes.

The force effect of the blade acting on the shaft can be decomposed into 2 perpendicular components. This decomposition into real and imaginary coordination is illustrated in Figure 1 left. The decomposition can be done for each blade vibration. The contribution of each blade in both coordinates can be summed into the total so-called asymmetry of blisk vibration. This represents the Equation 1.

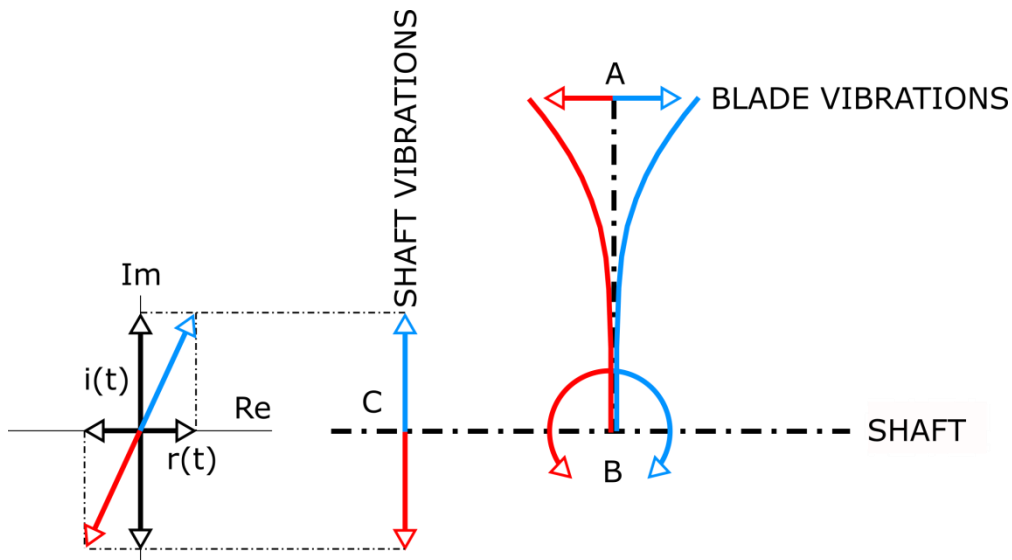


Figure 1: Blade propagation into shaft vibration and decomposition in shaft cross-section

$$ir(t) = r(t) + j \cdot i(t) = R \cos(2\pi f_b t + \varphi_R) + j \cdot I \sin(2\pi f_b t + \varphi_I) \quad (1)$$

Equation 1 represents elliptic trajectory in general. According to McConnell and Varoto (1995), elliptic trajectory can be decomposed into 2 counter rotating circular phasors. This represents Equation 2. The principle of the decomposition is illustrated in the Figure 2.

$$ir(t) = A_F e^{j(2\pi f_b t + \phi_F)} + A_B e^{j(-2\pi f_b t + \phi_B)} \quad (2)$$

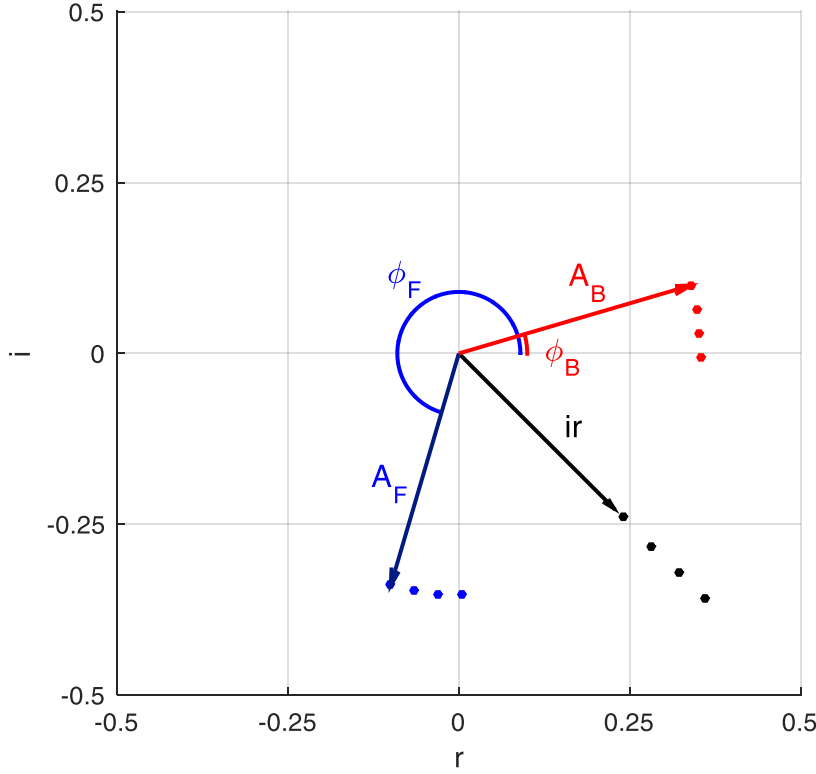


Figure 2: Ellipse decomposition into counter rotating phasors

Equation 1 and Equation 2 can be put together as Equation 3.

$$R \cos(2\pi f_b t + \phi_R) + j \cdot I \sin(2\pi f_b t + \phi_I) = A_F e^{j(2\pi f_b t + \phi_F)} + A_B e^{j(-2\pi f_b t + \phi_B)} \quad (3)$$

Euler formula can be applied on left side of Equation 3 leading to Equation 4.

$$ir(t) = \frac{R}{2} [e^{j(2\pi f_b t + \phi_R)} + e^{-j(2\pi f_b t + \phi_R)}] + \frac{jI}{2j} [e^{j(2\pi f_b t + \phi_I)} - e^{-j(2\pi f_b t + \phi_I)}] \quad (4)$$

Members of Equation 4 can be rearranged into Equation 5.

$$ir(t) = e^{j2\pi f_b t} \left[\frac{R}{2} \cdot e^{j\phi_R} + \frac{I}{2} \cdot e^{j\phi_I} \right] + e^{-j2\pi f_b t} \left[\frac{R}{2} \cdot e^{-j\phi_R} - \frac{I}{2} \cdot e^{-j\phi_I} \right] \quad (5)$$

Forward rotating phasor given by Equation 5 can be compared with the first right side member of Equation 2 leading into Equation 6. The same can be done in case of backward rotating phasor and the second side member of Equation 2 resulting in Equation 7.

$$A_F e^{j\phi_F} = \frac{R}{2} \cdot e^{j\phi_R} + \frac{I}{2} \cdot e^{j\phi_I} \quad (6)$$

$$A_B e^{j\phi_B} = \frac{R}{2} \cdot e^{-j\phi_R} - \frac{I}{2} \cdot e^{-j\phi_I} \quad (7)$$

Euler's formula can be applied on Equation 6 and 7 leading into Equation 8 and 9, respectively.

$$A_F e^{j\varphi_F} = (R \cos \varphi_R + I \cos \varphi_I) + j(R \sin \varphi_R + I \sin \varphi_I) \quad (8)$$

$$A_B e^{j\varphi_B} = (R \cos \varphi_R - I \cos \varphi_I) + j(R \sin \varphi_R - I \sin \varphi_I) \quad (9)$$

The amplitude of forward rotating phasor can be expressed by Equation 10 by transferring the right side of Equation 8 into a polar form using Pythagorean identity and the cosine of a difference. The same can be done for the amplitude of backward rotating phasor, see Equation 11.

$$A_F = \frac{1}{2} \cdot \sqrt{R^2 + I^2 + 2RI \cdot \cos(\Delta\varphi)} \quad (10)$$

$$A_B = \frac{1}{2} \cdot \sqrt{R^2 + I^2 - 2RI \cdot \cos(\Delta\varphi)} \quad (11)$$

The Equation 12 defines the phase difference from previous equations.

$$\Delta\varphi = \varphi_R - \varphi_I \quad (12)$$

The Equations 10 and 11 represent the amplitudes of counter rotating phasors of the co called asymmetry of blisk vibration, abbreviated as blisk asymmetry. The question is, in which form is the blisk asymmetry measured by the relative rotor vibration sensor. For this purpose, the rotational movement of the shaft must be included into the model. This reflects Equation 13 as the result of blisk asymmetry and clockwise rotating unit phasor multiplication. The rotational speed of this phasor equals the angular speed of the shaft. Using Equation 2, the Equation 13 can be rewritten into Equation 14.

$$ir_o(t) = ir(t) \cdot e^{j(2\pi f_o t + \varphi_o)} \quad (13)$$

$$ir_o(t) = A_F e^{j(2\pi(f_o + f_b)t + \varphi_F + \varphi_o)} + A_B e^{j(2\pi(f_o - f_b)t + \varphi_B + \varphi_o)} \quad (14)$$

Equation 14 illustrates the principle of blisk asymmetry propagation into the relative rotor vibration sensor. The presence of two spectral components is obvious and so the Equation 14 can be simplified into Equation 15. This equation corresponds to the spectral distribution in a form of two components as it was mentioned in introduction. LSB, USB represent lower sideband and upper sideband, respectively.

$$ir_o(t) = USB + LSB \quad (15)$$

EXPERIMENTS

The theory described in previous chapter must be validated by an appropriate experiment. For this purpose the experimental rotor test rig SpectraQuest Magnum was used. It consists of a 0,889 m long shaft with 0,019 m in diameter. The connection to the base is made by 2 lubricated sleeve bearings. The bearing distance is 0,724 m. For the experimental purposes the bladed disk - blisk - was designed. The blisk was made of 2 millimeter thick metal and was mounted into the middle of the shaft using 2 flanges. They were connected together with screws passing through each blade of the blisk. The eigenfrequency of each blade was thus possible to change by tightening the screw belonging to the blade. The installation of the blisk reflects Figure 3.

For the excitation of the blades the piezoelectric transducers were used. They were adherent to the blade roots with epoxy. In this experiment, 2 blades were excited to be able to ensure required blisk asymmetry. Distance between piezoelectric transducers was 90°. The module generating the

required harmonic voltage excitation of piezoelectric transducers was composed of a control microcomputer Atmega328 with Arduino Nano bootloader and communication RF module NRF24L01. The harmonic signal was generated by the AD9833 and amplified to voltage of ± 20 V. The digital potentiometer MCP4651-103E was used to control the gain. The logic part was powered by 5 V and 3.3 V. For this purpose 9V battery was used so the voltage was reduced by a linear stabilizer. The analog part was powered by ± 18 V from series of 9V batteries - each pair of batteries provides power to one piezoelectric transducer. This module, together with the batteries, was attached to the rotor to withstand the centrifugal force caused by the rotation. The installation of this module illustrates Figure 3.

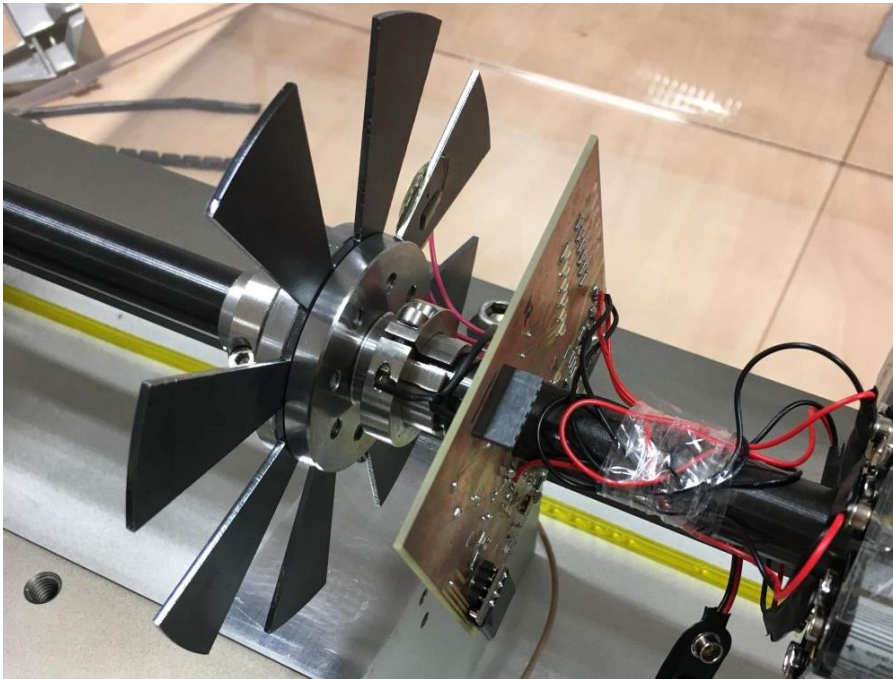


Figure 3: The receiver module generating the excitation of the blades

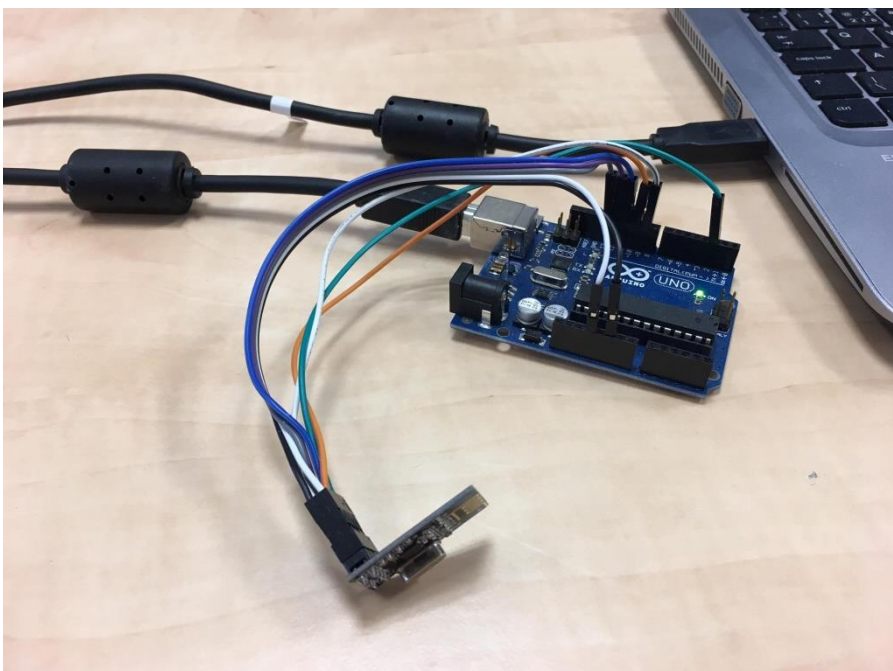


Figure 4: Transmitter module commanding the receiver module

To be able to command the above described module and set or change the required excitation parameters during rotation, the transmitter module was developed. This module is based on an Arduino Nano board with an Atmega328 and Wi-Fi module NRF24L01. The LabView platform was used to make a GUI to control the transmitter module via USB and communicate and command the module that generates the blade excitation. The transmitter module is in Figure 4.

The sensors of relative rotor vibration signal Emerson PR 6422 were mounted on the bearing pedestal and wired through signal convertor CON 041 into NI 9234 and NI cDAQ-9139. The sensors are a non-contact eddy current transducers measuring shaft-sensor displacement in x-y arrangement. The sampling frequency was 25 kHz. The operational temperature range is $-35:180$ °C with less than 2 % error. These sensors meet ISO 10817-1 standard that defines measuring equipment for steam turbine vibration monitoring. In industrial practice PR 6423 sensor is used, which is the same series sensor as PR 6422, only the measuring range is 2 mm and sensitivity 8 V/mm unlike PR 6422 case where the measuring range is 1 mm and sensitivity 16 V/mm.

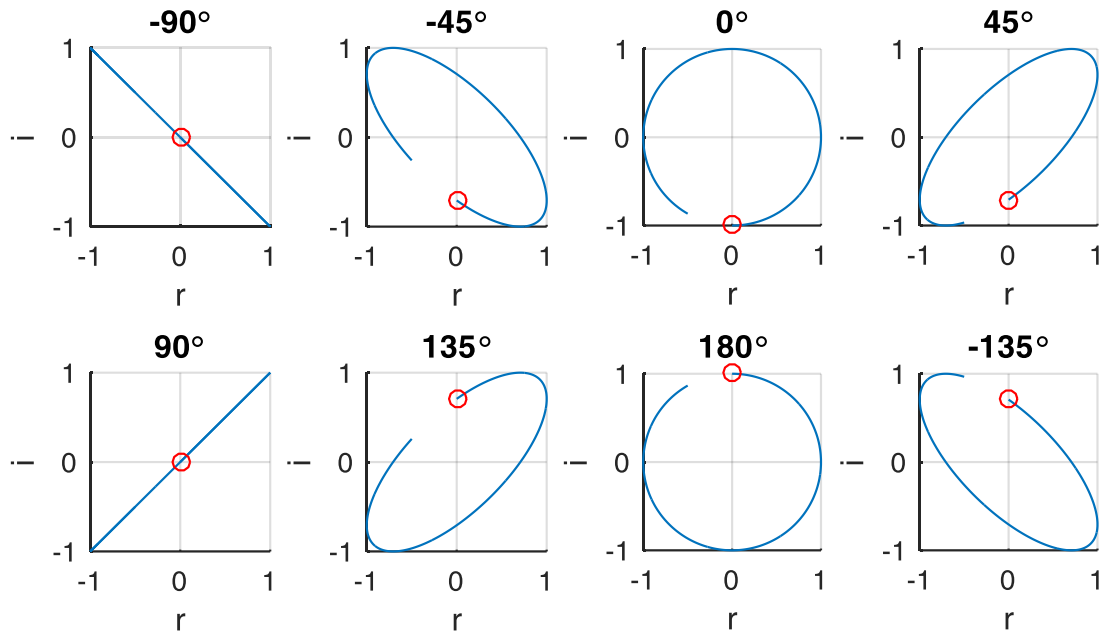


Figure 5: Examples of blisk vibration asymmetry excitation in experiment

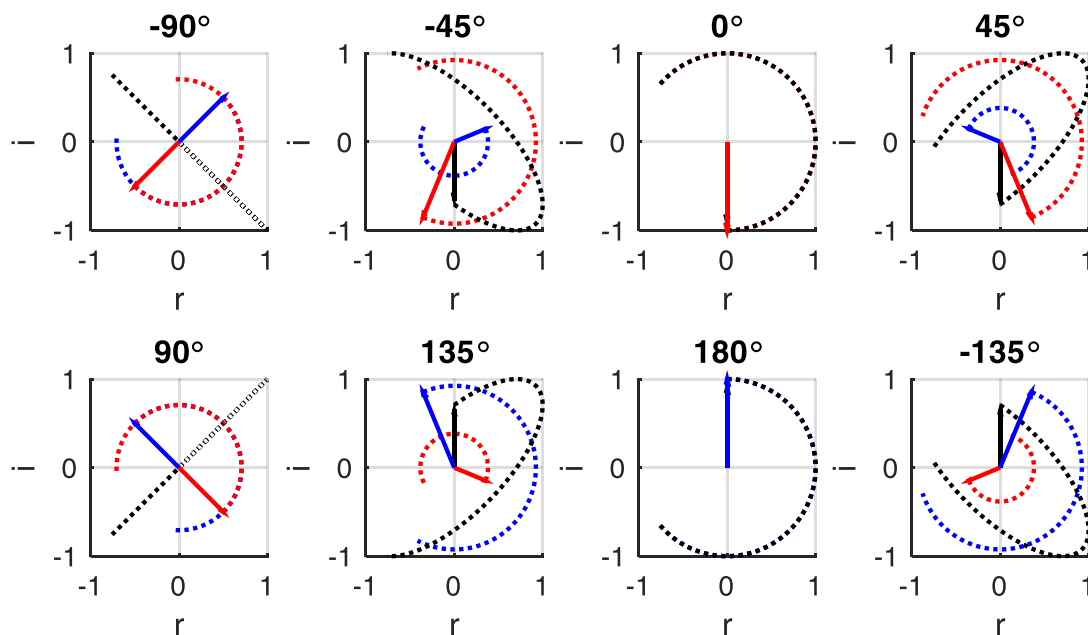


Figure 6: Decomposition of experimental asymmetries into counter rotating phasors

As it was described in theory chapter, the amplitudes of USB and LSB represent amplitudes of forward and backward rotating phasors defined by formulas 10 and 11, respectively. An experiment was set up to verify these formulas.

The transmitter and receiver modules were used to generate the required excitation of the blisk according to the Figure 5. Eight configurations of the blisk excitation used in this experiment are illustrated there. The variable parameter was in this case the phase difference according to Equation 12. The amplitudes R and I were set to be unit.

Each blisk asymmetry from Figure 5 was decomposed into 2 counter rotating circular phasors according to Equation 2. The result of this decomposition is in Figure 6. Forward rotating phasor is represented by red color and backward rotating phasor is represented by blue color. The amplitudes of these phasors should be compared with LSB and USB amplitudes identified from relative rotor vibration signal spectrum to found out if theoretical equations correspond to the measurement. The rotational frequency was 20 Hz in this experiment.

RESULTS

The comparison of theoretical and experimental values identified by the measurement is illustrated in Figure 7. The red dashed line represents theoretical dependence of USB amplitude on phase difference defined by formula 10. The blue dashed line represents theoretical LSB amplitude. Relative rotor vibration signal was measured for each blisk asymmetry excitation described in previous chapter. The discrete Fourier transform was applied to the signal and USB and LSB components were identified from the spectrum. The identified amplitudes of USB and LSB are illustrated in the Figure 7 in form of squares. It can be easily discovered that the theoretical and experimental values are well correlated. It proves that the blade behavior follows the equations described in theory background chapter.

Based on the result of the previous experiment, 3 additional measurements of the relative rotor vibration were captured and processed by the discrete short-time Fourier transform - DSTFT (Boashash 2005). The measurement was made for the runup of the rotational frequency from 0 to 1200 RPM. In Figure 8 there is DSTFT of the first measurement for case $\Delta\phi = 90^\circ$ and so the LSB and USB amplitudes should be equal. In Figure 9 there is DSTFT of the measurement for case $\Delta\phi = 0^\circ$ that should result in zero LSB amplitude while USB amplitude is at its maximum. In the Figure 10 there is DSTFT of the measurement for case $\Delta\phi = 180^\circ$ that should result in zero USB amplitude while LSB amplitude is at its maximum. These experiments follow the theory described in this paper as well.

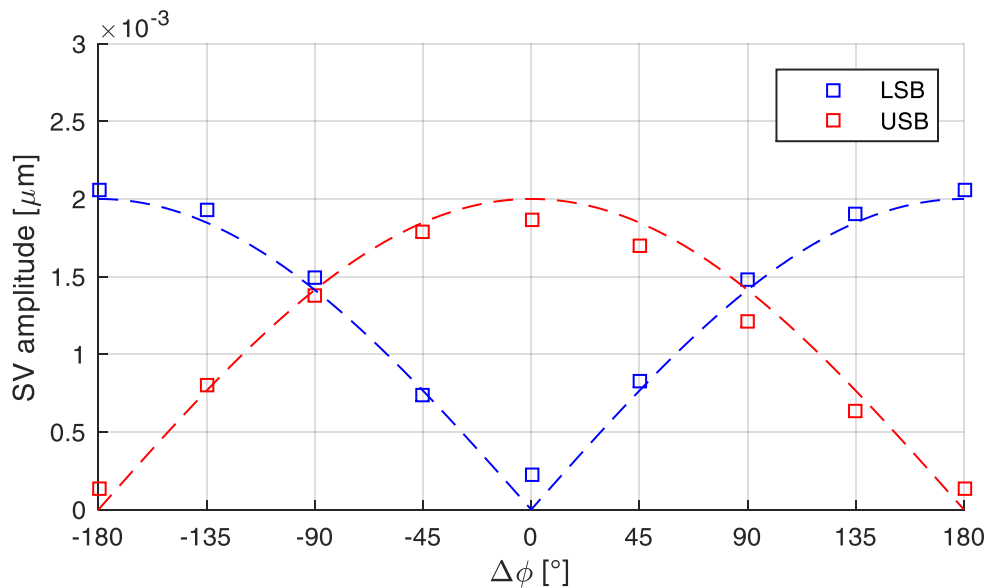


Figure 7: Experimental and theoretical result comparison

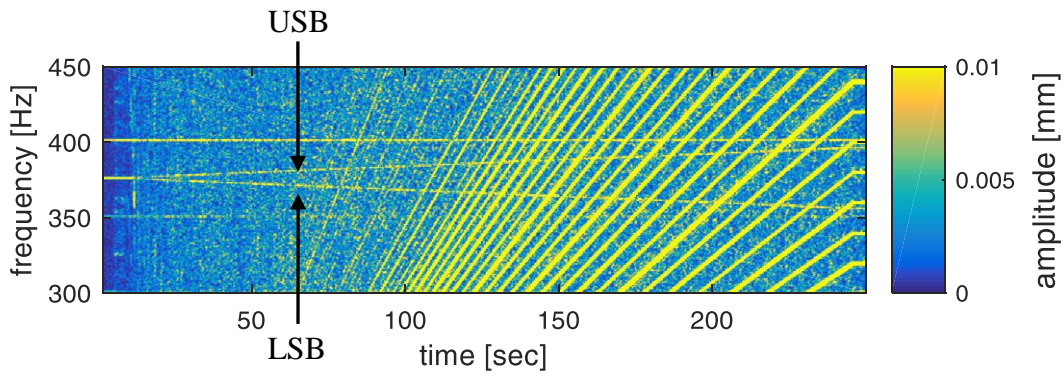


Figure 8: DSTFT of relative shaft vibration signal in case phase difference is 90°

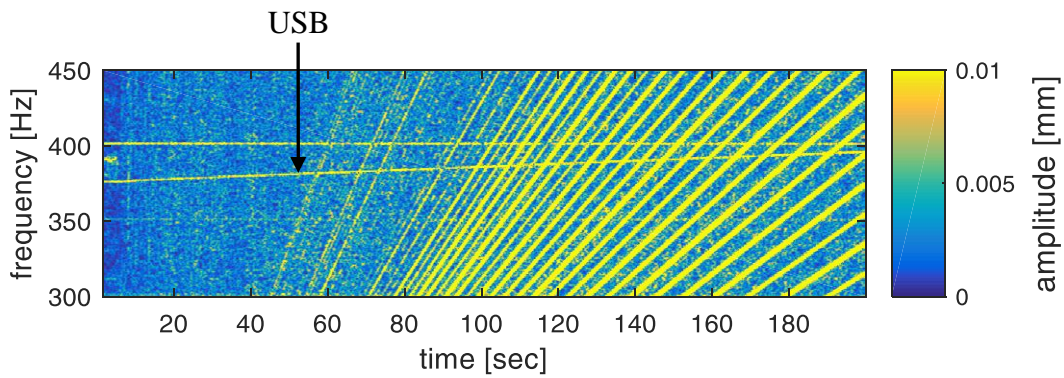


Figure 9: DSTFT of relative shaft vibration signal in case phase difference is 0°

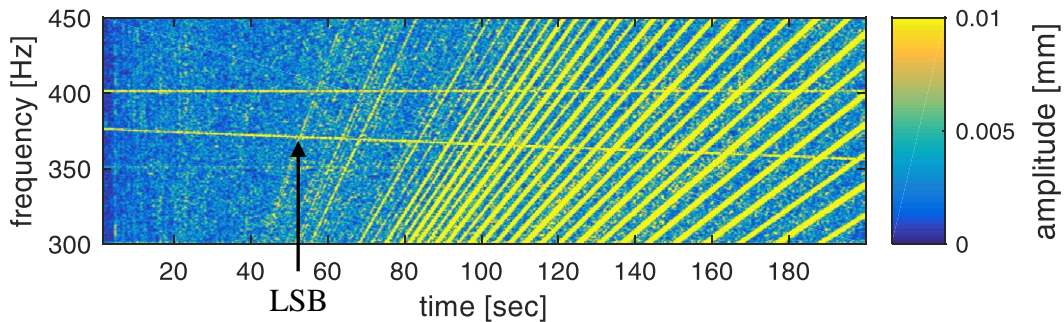


Figure 10: DSTFT of relative shaft vibration signal in case phase difference is 180°

CONCLUSIONS

In previous papers, the methods for identification of dynamic behavior of the blades using the relative rotor vibration signals were introduced. For example the identification of the blade eigenfrequencies from the relative rotor vibration signals can be used for building the operational Campbell diagram of the blades. This was achieved from the knowledge of the spectral distribution of the blade vibration presented in relative rotor vibration signal in form of 2 spectral components – LSB and USB. For building the operational Campbell diagram of the blades the frequencies of LSB and USB are being used. The idea which was at the beginning of this paper research was to use also the amplitudes of LSB and USB for blade state diagnostics. However the understanding of the exact meaning of the amplitudes was necessary at first.

The principle of how the blade vibration is being transmitted into the relative rotor vibration is described in detail in the theory background chapter. In the experiments chapter the experimental rotor test rig was introduced together with designed blisk and its excitation using piezoelectric

transducers controlled by modules with wireless communication. The theoretical values of LSB and USB amplitudes are obtained in this chapter as well.

The results of the LSB and USB amplitude identification from relative rotor vibration signals measured on test rig are presented in the following chapter. The comparison of experimental and theoretical results is presented in this chapter as well. There can be seen that both well corresponds together validating the theory background of this paper.

The most important benefits of this research are the consequences based on the results presented in this paper. The blade state monitoring can be done using only the amplitudes of LSB and USB. However the choice of the indicator was not obvious till today.

The suitable indicator reflecting any blisk dynamic change may be the ratio of USB and LSB amplitude - A_F/A_B . Let's imagine the real situation, when the blades of the steam turbine are installed and operated. The vibration of the blades can be put together in the so-called blisk asymmetry. This asymmetry is nonzero in general, because the ideal manufacturing in real does not exist. The blisk asymmetry can be considered as a signature of the bladed disk dynamic action on the shaft. According to the steam flow velocity, pressure etc. the forces acting on blades can vary in time, that cause the blades vibrate with higher amplitudes, but together they do the same signature, which is scaled only. According to this, amplitudes of LSB and USB will proportionally raise but A_F/A_B will remain constant. Contrary to this, if any of the blades changes its natural dynamic behavior, it will also lead in a change of the overall blisk signature – asymmetry – accompanied with the change of A_F/A_B .

This paper comes with the new possibility of the blade state monitoring using LSB and USB amplitudes identified from relative rotor vibration. The future research will be focused on the use of LSB and USB phases for further diagnostic purposes that could help to localize and identify the blade that changed its dynamic behavior during operation.

To be able to use this approach, the blade vibration components must be above the noise level in the shaft vibration signal, thus the sensor must not be under the node of the shaft standing wave. That situation is shown for example in Jakl et al. (2020).

ACKNOWLEDGEMENTS

This work was supported from ERDF under project "Research Cooperation for Higher Efficiency and Reliability of Blade Machines (LoStr)" No. CZ.02.1.01/0.0/0.0/16_026/0008389.

REFERENCES

Boashash, B., (2005). Time frequency signal analysis and processing, A comprehensive reference. Elsevier Ltd, ISBN 978-0-08-044335-5

Jakl, J., Liska, J., Vasicek, V., (2020). *Usage of shaft vibration signals for turbine blades monitoring*. Condition Monitor, Issue 401, August 2020. Northampton, UK. ISSN 0268-8050

Liska, J., Vasicek, V., Jakl, J., (2018). *On possibilities of using relative shaft vibration signals for rotating blades monitoring*. Proceedings of ASME Turbo Expo 2018, Turbomachinery Technical Conference and Exposition, Oslo, Norway

McConnell, K. G., Varoto P. S., (1995). *Vibration Testing: Theory and Practice*. John Wiley & Sons

Peng, W. W., (2007). *Fundamentals of Turbomachinery*. John Wiley & Sons, Inc., Hoboken, New Jersey, USA, ISBN: 978-0-470-12422-2

Vasicek, V., Liska, J., Strnad, J., Jakl, J., (2019). *Experimental validation of the blade excitation in a shaft vibration signals*. Proceedings of the Second World Congress on Condition Monitoring – WCCM, 2-5 December, 2019. Singapore. ISBN 978-981-11-0744-3

Zilly, A., (2014). *Entwicklung einer Bewertungsmethodik für mit betrieblichen Wellenschwingungssensoren gemessene Schaufelschwingungen*. Betreuer Dipl.-Ing. J. Funcke, Dr.-Ing. D. Bloemers. Fakultät für Maschinenwesen Institut für Kraftwerkstechnik, Dampf- und Gasturbinen, Aachen, März. Diplomarbeit